The Endoscopic Endonasal Approach to Craniovertebral Junction Pathologies: Surgical Skills and Anatomical Study

Paolo Pacca, Valentina Tardivo, Giancarlo Pecorari, Diego Garbossa, Alessandro Ducati, and Francesco Zenga

Abstract *Introduction:* Surgical anterior decompression is the treatment of choice for symptomatic irreducible ventral craniovertebral junction (CVJ) compression. Along with the classic transoral approach, the endoscopic endonasal approach has evolved and is gaining growing success.

Materials and Methods: In this work we discuss the surgical technique, give a complete step-by-step description of dissection of the craniovertebral junction and report a specific case of endoscopic endonasal odontoidectomy with use of a high-definition (HD) three-dimensional (3D) endoscope.

Discussion: The extended endonasal approach exploits an anatomical corridor to the odontoid process, involving only a small incision in the nasopharynx and sparing palate integrity. The most important limitation of the technique is 2D visualization, which hinders correct recognition of anatomical structures.

Conclusion: The endoscopic endonasal route to the odontoid process has proven to be a feasible, safe and well-tolerated procedure. Anatomical study is very important for better understanding of the 3D anatomy of the CVJ and relation of critical neurovascular structures to specific bony and muscular landmarks.

Keywords Odontoidectomy · Endoscopic · Endonasal approach · CVJ stability · Anatomical study

P. Pacca (✉)
Division of Neurosurgery, Department of Neurosciences, University of Turin, Turin, Italy

SC Neurochirurgia U, Presidio Molinette Dipartimento di Neuroscienze e Salute Mentale, Città della Salute e della Scienza, Turin, Italy

V. Tardivo · D. Garbossa · A. Ducati · F. Zenga
Division of Neurosurgery, Department of Neurosciences, University of Turin, Turin, Italy

G. Pecorari
1st ENT Division, Department of Surgical Sciences, University of Turin, Turin, Italy

Introduction

The craniovertebral junction (CVJ) is a complex transition area between the skull and the upper cervical spine, and it provides stability and motion [1–3]. Biomechanical studies have confirmed that the majority of spine flexion, extension and rotation occur at this level [4–6]. Moreover, vital neurological and vascular structures are housed in the CVJ. Different pathologies may affect the CVJ, leading to impairment/limitation of its physiological function with loss of mobility and eventually compression of neurovascular structures. Prompt surgical intervention is required when these disorders cause symptomatic high spinal cord or brainstem compression. Focusing on the pathology of the odontoid process, if such disorders are not treated, they may cause ventral brainstem and spinal cord compression with subsequent neurological deficits. In addition, if the ligaments are disrupted (especially the transverse ligament), instability and subassial atlo-occipital dislocation may occur. Rheumatoid arthritis, metastasis and congenital deformities represent the most frequent disorders involving the CVJ and the odontoid process [7]. In cases of irreducible ventral compression at the CVJ, anterior approaches offer direct access to the lesion without the need for neural tissue retraction, with a consequently low rate of lower cranial nerve injury [8]. Along with the classic transoral approach, the endoscopic endonasal approach has evolved and is gaining growing success. The latter, in fact, has been shown to be safe and effective, avoiding the need for tongue retraction, upper airway swelling, and the need for palate splitting [9]. The surgical field has anatomical limits dictated by the osseous structures of the region (the nasal and palatine bones), which form two lines: the Kassam line and the naso-axial line, which define a triangle-shaped surgical corridor [10]. The most important limitation of the technique is two-dimensional (2D) visualization, which hinders correct recognition of anatomical structures. The high-definition (HD) 3D endoscope is a new instrument that overcomes this problem, thus giving the transnasal approach enormous and growing

importance in surgery in this region [11, 12]. This paper discusses our experience with the extended endoscopic endonasal approach (EEA) to the craniovertebral junction, using a specific case to provide a complete step-by-step description of the surgical technique used for the dissection, and discusses the advantages and limitations of this approach.

Dissection

Access to the foramen magnum and the CVJ requires a low trajectory in comparison with sellar approaches [13]. The posterior nasal septum, inferior sphenoid wall and vomer are removed so the rhinopharyngeal part of the clivus can be reached [14]. The inferior third of the clivus is drilled away to improve the exposure of anterior CVJ. The lateral limits of the exposure are determined by the carotid protuberance, foramen lacerum, vidian canal and Eustachian tube. The nasopharyngeal mucosa is removed, widely exposing the underlying basipharyngeal fascia and the median raphe covering the prevertebral muscles (Fig. 1). Two muscles cover this area anterior to the foramen magnum and extend from the clivus downward: the longus capitis and rectus capitis anterior (RCpA). The longus capitis is removed and has multiple bellies (Fig. 1). The atlanto-occipital membrane (AOM) is a broad fibrous structure, which extends from the anterior edge of the foramen magnum to the superior edge of the anterior arch of the atlas (Fig. 2). The median raphe is a band of connective tissue, which is attached to the clivus and continues as the anterior longitudinal ligament (Fig. 2). It is necessary to remove the AOM and the anterior median raphe to expose the foramen magnum and the anterior arch of C1 (Fig. 3). The alar and
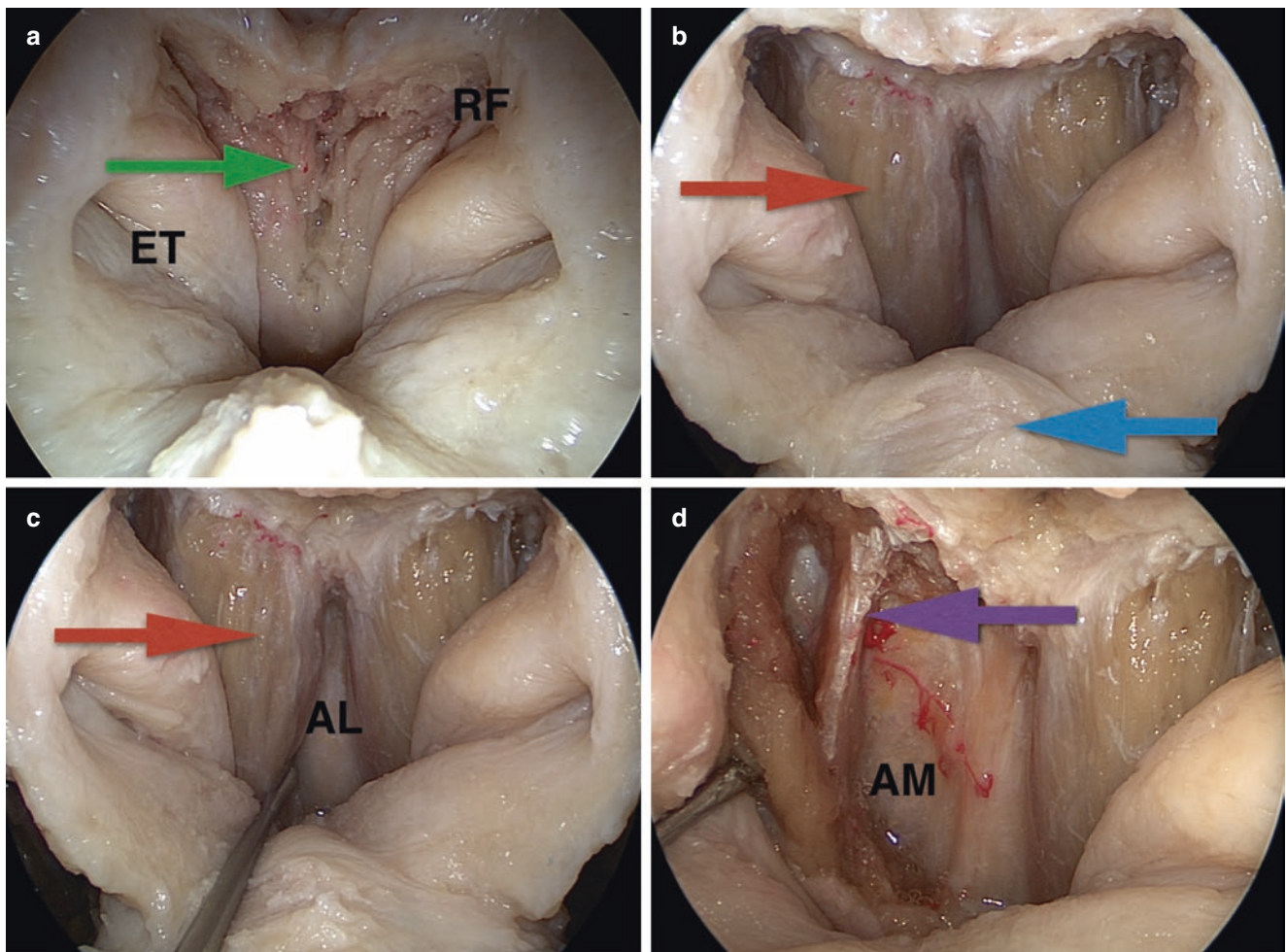

Fig. 1 Stepwise endoscopic approach to the foramen magnum and craniovertebral junction. (**a**) View of the mucosa of the rhinopharynx (*green arrow*) with the Eustachian tubes (ET) and the fossa of Rosenmüller (RF) as the lateral limits of this exposure. (**b**) Floor of the nasal cavity (*blue arrow*). The nasopharyngeal mucosa has been removed, exposing the basipharyngeal fascia overlying the longus capitis muscle (*red arrow*) and the median raphe attached to the pharyngeal tubercle on the midline (AL). (**c**) The longus capitis muscle (*red arrow*) can be seen after removal of the fascia. It is attached laterally to the pharyngeal tubercle along the superior clival line. (**d**) The longus capitis muscle has multiple bellies and is attached in layers to the clivus, as can be seen after partial removal from the right side (*purple arrow*). (AM) anterior atlantooccipital membrane
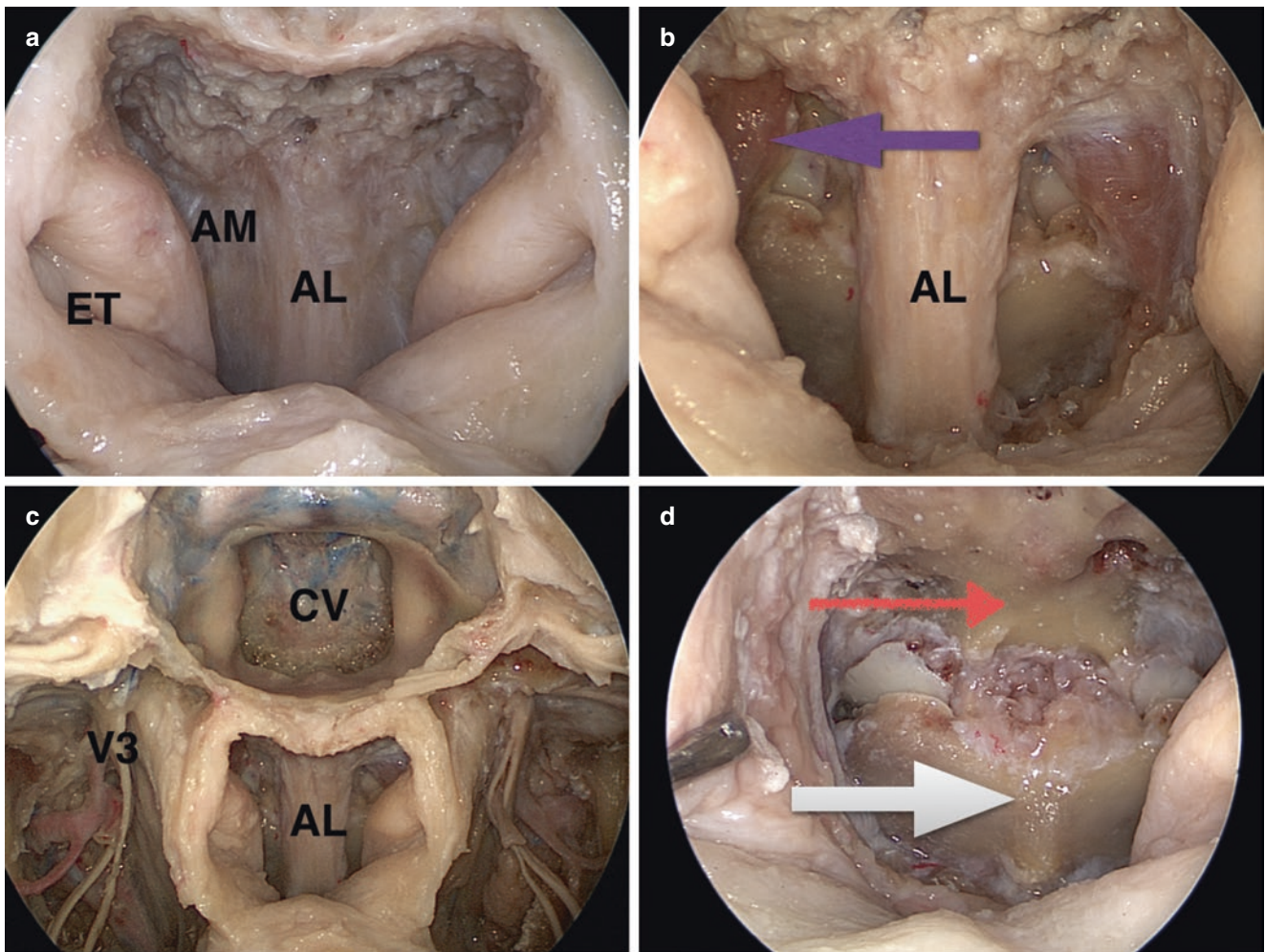
Fig. 2 Stepwise endoscopic approach to the foramen magnum and the craniovertebral junction. (**a**) Both sides of the longus capitis are removed, exposing the median raphe part of the anterior longitudinal ligament (AL) attached to the pharyngeal tubercle and laterally forming a thick, broad membrane called the anterior atlanto-occipital membrane (AM). (**b**) Both the longus capitis and the anterior atlanto-occipital membrane have been removed, exposing the anterior longitudinal ligament on the midline (AL) and the atlanto-occipital joint. The rectus capitis anterior muscle can be seen laterally attached along the clivus from the inferior clival line to the foramen magnum (*purple arrow*).

(**c**) Extended endonasal approach to the clivus (CV); the sphenoid stage of dissection has been completed. On the right side, the infratemporal fossa has been dissected, showing the path of the Eustachian tube and the branches of the mandibular nerve in depth (V3). (**d**) The anterior longitudinal ligament and rectus capitis anterior have also been removed here, exposing the foramen magnum and the arch of C1 with both atlanto-occipital joints (*white arrow*). The gap between the C1 arch and the foramen magnum is filled with dense connective tissue, which also encloses the apical and alar ligaments attached to the dens of C2. The pharyngeal tubercle can be seen here (*red arrow*)

apical ligaments are located within the space between the foramen magnum and the anterior arch of C1. To view the odontoid process and the ligaments it is necessary to partly remove the anterior arch of C1 (Fig. 3). The atlas has two lateral masses: an anterior arch with a midline anterior tubercle, and a posterior surface (Fig. 3). The alar ligaments are fibrous bands arising from the lateral surface of the odontoid process and ascending toward the alar tubercle on the medial side of the occipital condyles (Fig. 3). The apical ligament of the odontoid process has a cartilaginous base arising from the apex of the dens and coming up to the anterior edge of the foramen magnum. The posterior surface of the dens also has a posterior facet, which articulates

with the cartilaginous facet on the anterior surface of the cruciform ligament (Fig. 4). The anterior cortical surface and the core of the dens are drilled, leaving only a thin shell of bone, which can be removed with rongeurs. Removal of the dens exposes a thick, strong, white band called the transverse ligament, which arches posteriorly the dens and holds it in position. It extends from the tubercles on the medial side of the lateral mass of the atlas (Fig. 4). The transverse ligament is the horizontal part of the cruciform ligament, which has two upper and lower vertical bands. The tectorial membrane, a broad fibrous band that spans the area between the medial edges of the occipital condyles, is a rostral extension of the posterior longitudinal ligament,
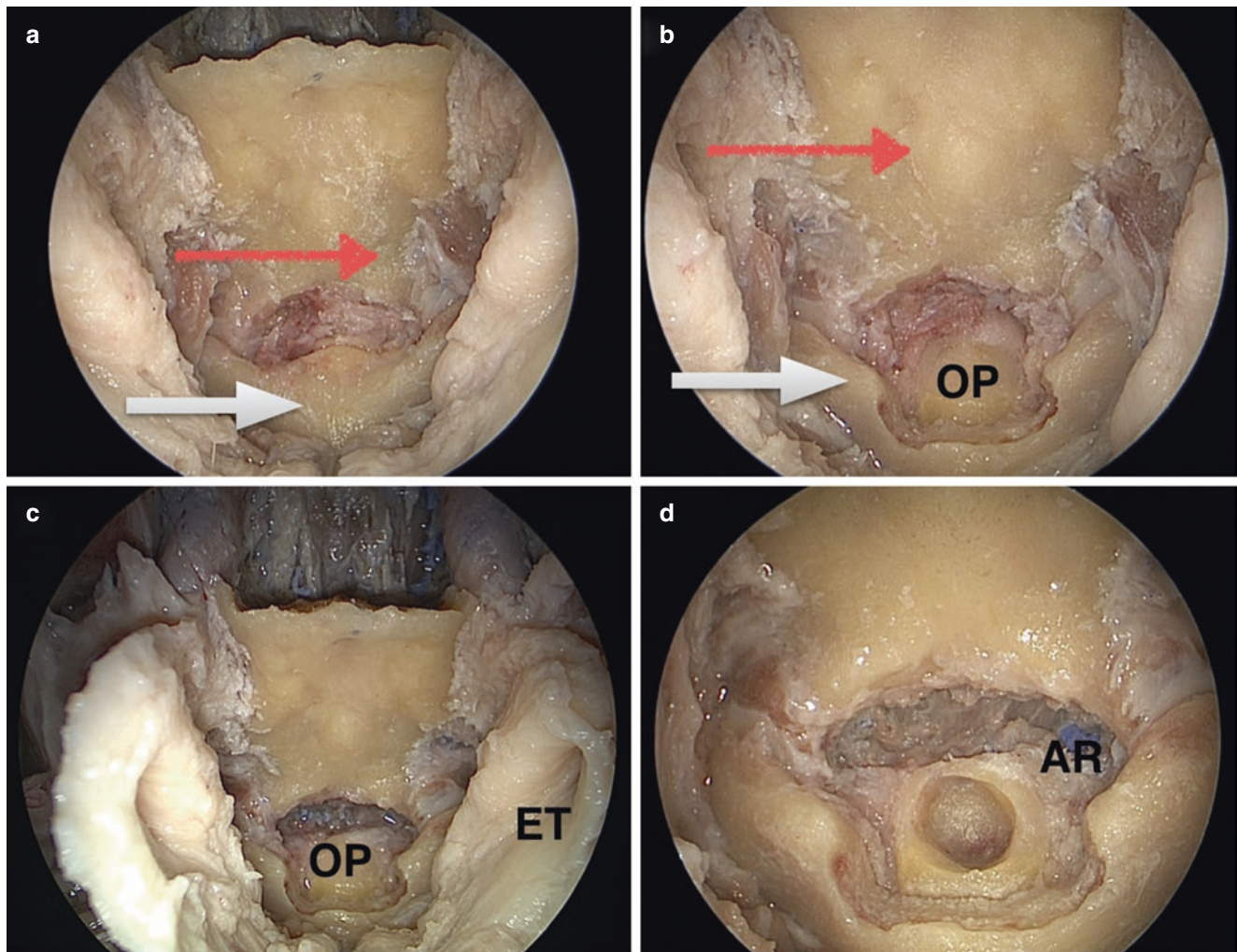
Fig. 3 Stepwise endoscopic approach to the foramen magnum and craniovertebral junction. (**a**) The foramen magnum after removal of the anterior longitudinal ligament and the anterior atlanto-occipital membrane. The supracondylar groove can be identified laterally with the rectus capitis anterior muscle (*red arrow*). (**b**, **c**) The clivus after removal of the muscles, showing the superior and inferior clival lines (*red arrow*). The inferior clival line corresponds to the supracondylar groove laterally. The anterior arch of C1 is partly removed (*white arrow*), exposing the odontoid process (OP). (**d**) The alar ligaments (AR), which are thick fibrous bands that attach to the posterolateral roughened surface of the odontoid process and ascend obliquely and laterally to attach the alar tubercles located on the medial side of the occipital condyles. Odontoidectomy begins with drilling of the central core, as seen here

which attaches to the axis inferiorly and the clivus superiorly (Fig. 4). It is separated from the dura by the epidural venous plexus. Once the dura is opened, the junction of the spinal canal with the medulla, which is defined as being at the level of the origin of the C1 ventral root, is exposed.

Case Illustration

The patient was a 71-year-old woman affected by an odontoid lesion. Because of radiological evidence of C1 myelopathy associated with both lower and upper limb weakness, she had undergone posterior C1–C2 laminectomy in November 2010 at another hospital.

After some months of disease stability she experienced worsening of limb weakness, with development of spastic paraparesis and gait impairment. Her reflexes were overreactive. She also complained of paraesthesia. Brain–cervical spine magnetic resonance imaging (MRI) (Fig. 5a, b) and computed tomography (CT) scanning (Fig. 6a, b) were performed. The radiological exams showed worsening of myelopathy without lesion growth.

Therefore, the patient underwent endoscopic endonasal odontoidectomy. The surgical procedure was uneventful, and postoperative CT scanning confirmed the success of the procedure. After 1 week a posterior C0–C2 arthrodesis was performed with an occipital plate and a C2 transcortical screw. Another cervical spine CT scan was performed to check for correct screw positioning.
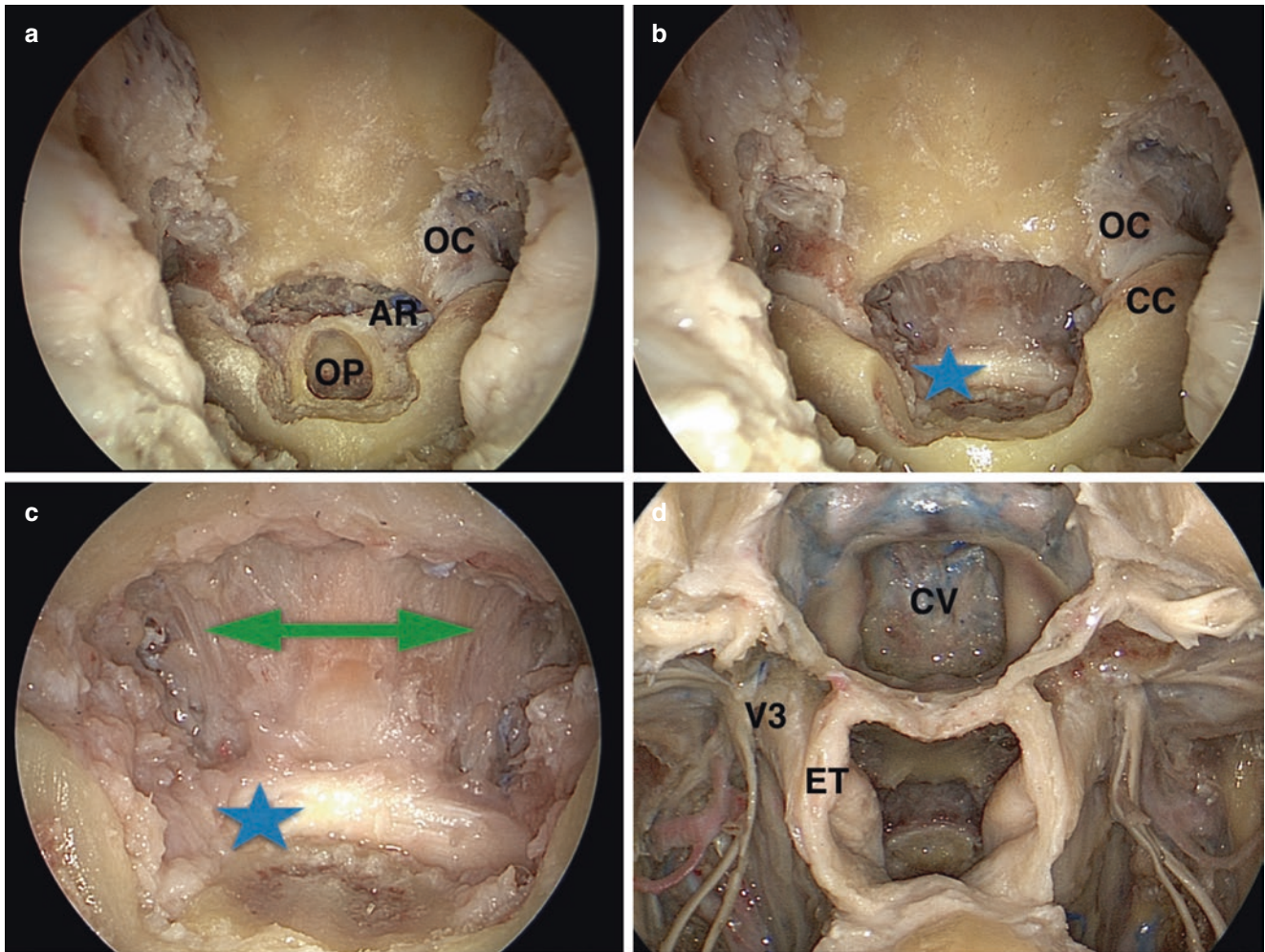
Fig. 4 Stepwise endoscopic approach to the foramen magnum and craniovertebral junction. (**a**) The alar ligaments (AR), which are thick fibrous bands that attach to the posterolateral roughened surface of the odontoid process and ascend obliquely and laterally to attach the alar tubercles located on the medial side of the occipital condyles (OC). Odontoidectomy begins with drilling of the central core, as seen here (OP). (**b**, **c**) Once the dens is removed, the transverse ligament (*blue star*) can be seen extending between the transverse tubercles on the medial side of the C1 lateral masses (CC). The tectorial membrane (*green arrow*) can be seen extending from the transverse ligament (*blue star*) to the foramen magnum. (**d**) Final image of the extended endonasal approach to the clivus (CV) when the sphenoid stage of dissection has been completed. The right and left infratemporal fossae have been dissected, showing the path of the Eustachian tube (ET) and the branches of the mandibular nerve in depth (V3). Complete dissection of the craniovertebral junction has been performed

The hospital stay was uneventful, and the patient was discharged after the second surgery. The histological diagnosis was an odontoid G2 chondrosarcoma. An intensive rehabilitation programme was useful to help the patient to reduce her gait impairment. MRI (Fig. 5c, d) and CT scans (Fig. 6c, d) were performed postoperatively, showing complete decompression of the dura. After 6 months a large area of arthrodesis was evident.

Surgical Technique

The procedure was performed with the assistance of neurophysiological monitoring. Somatosensory and motor-evoked potential data were collected for the patient. The surgical team was composed of a neurosurgeon and an ear, nose and throat surgeon. The surgery was done with a Visionsense III, 3D endoscope (Visionsense Ltd, Petach Tikva, Israel). Everyone in the surgical theatre wore passive polarized glasses to obtain a stereoscopic view [15, 16].

The patient was placed in a supine position with the head fixed in a three-pin head holder (Mayfield Infinity Skull Clamp; Integra LifeSciences Corporation. We positioned the head slightly tilted to the left on the coronal plane and slightly flexed to slide up the dens. All positioning manoeuvres were performed under neurophysiological monitoring. The nasal cavities were prepared preoperatively with 2 mL of 10% carbocaine (mepivacaine) with adrenaline, which was applied topically with patties. A binostril 4-hand technique was used routinely. Once the surgeons entered the
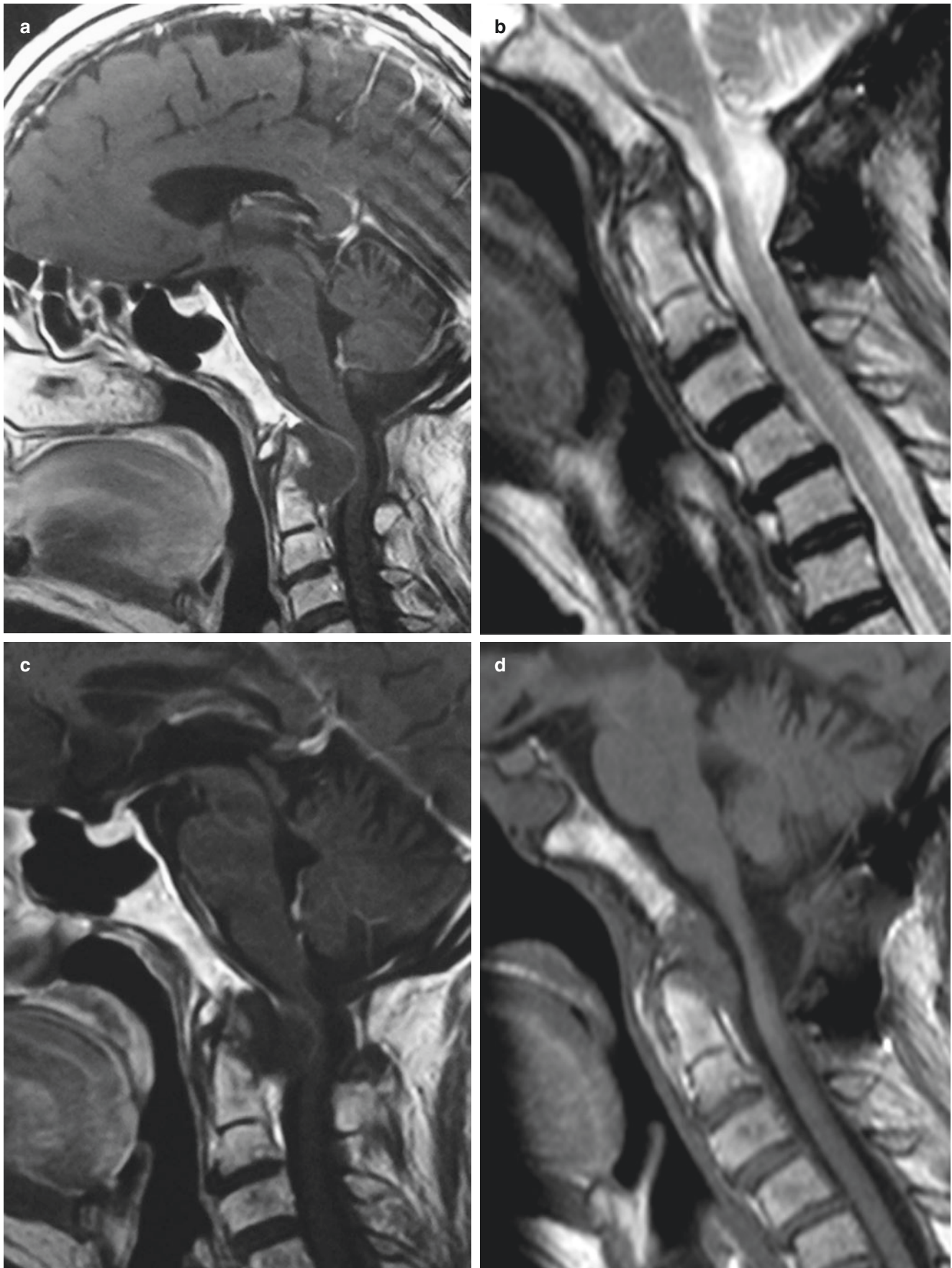
Fig. 5 (**a**, **b**) Preoperative magnetic resonance image (MRI) showing a complex craniovertebral junction malformation with a lesion of the odontoid process. (**c**, **d**) Postoperative MRI showing good spinal cord decompression

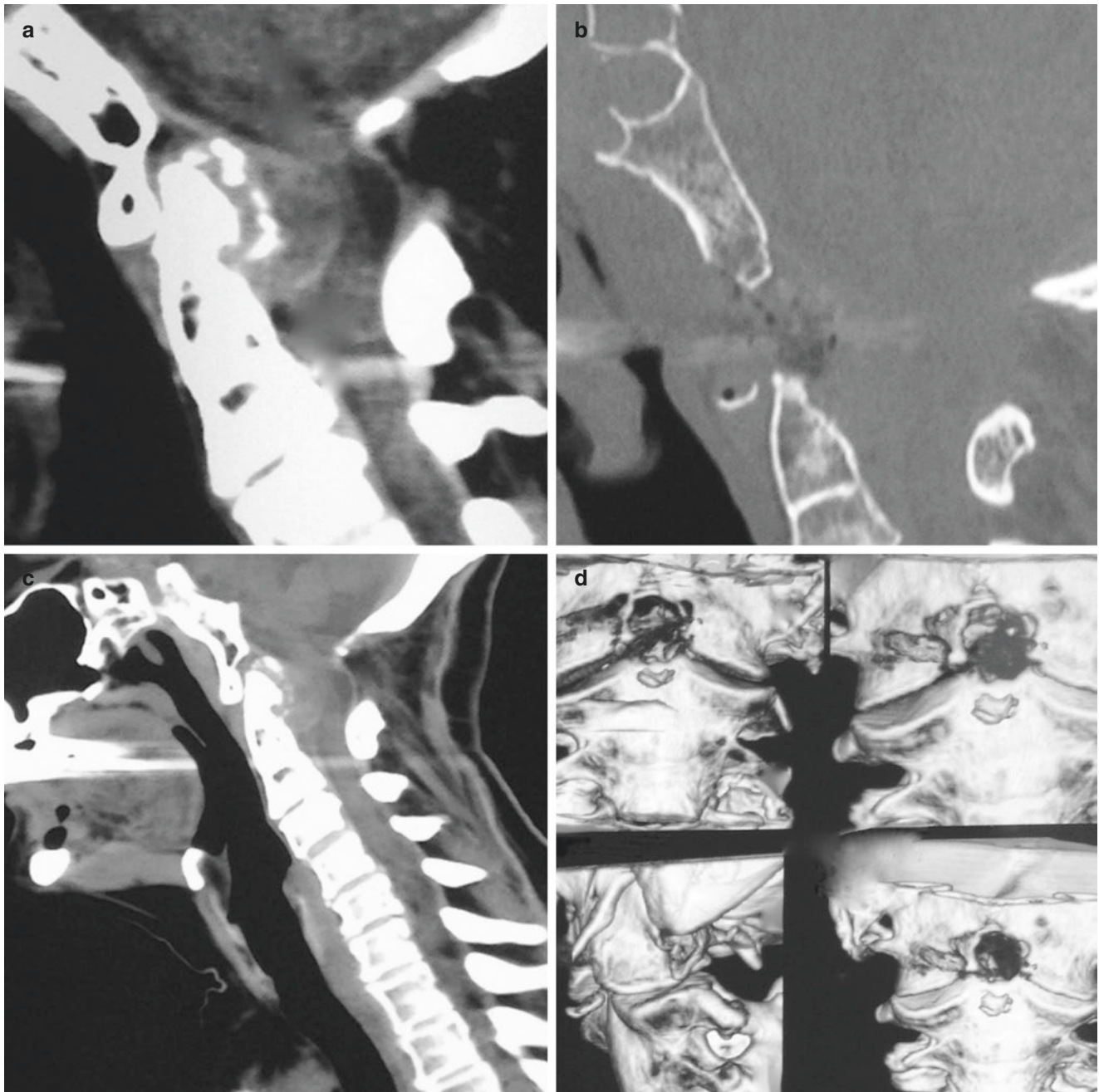**Fig. 6** (**a**, **b**) Preoperative computed tomography (CT) scan showing a complex craniovertebral junction malformation with a lesion of the odontoid process. (**c**, **d**) Postoperative CT scan showing good bone decompression

right nostril, the inferior and middle turbinates were displaced laterally to widen the surgical corridor (Figs. 7 and 8). The inferior margin of the middle turbinate, the nasopharynx, and the Eustachian tubes were the surgical landmarks that led the surgeons to the craniocervical junction. We usually do not remove the turbinates to preserve physiological airflow. The inferior margin of the middle turbinate was then followed until the nasopharyngeal cavity was entered. To enable use of both nostrils, the posterior third of the nasal septum was removed (Fig. 9). The junction between the clivus and the atlas was grossly defined by a line connecting the Eustachian tubes. The anatomical boundaries of the surgical field were defined by the floor of the sphenoidal sinus superiorly, the upper part of the oropharynx inferiorly, and the Eustachian tubes and the fossa of Rosenmüller laterally. The neuronavigation system provided significant help for identification of the anatomy at this point, especially concerning the vertical tracts of the internal carotid arteries. An inverted U-shaped flap of nasopharyngeal mucosa and muscular layers was harvested with the laser (CH fibre laser; Dornier MedTech, Munich, Germany) (Fig. 9). The Eustachian tubes had to be considered the most lateral margin of the incision because they identified the parapharyngeal segment of the carotid artery. The craniocaudal extension of the flap involved
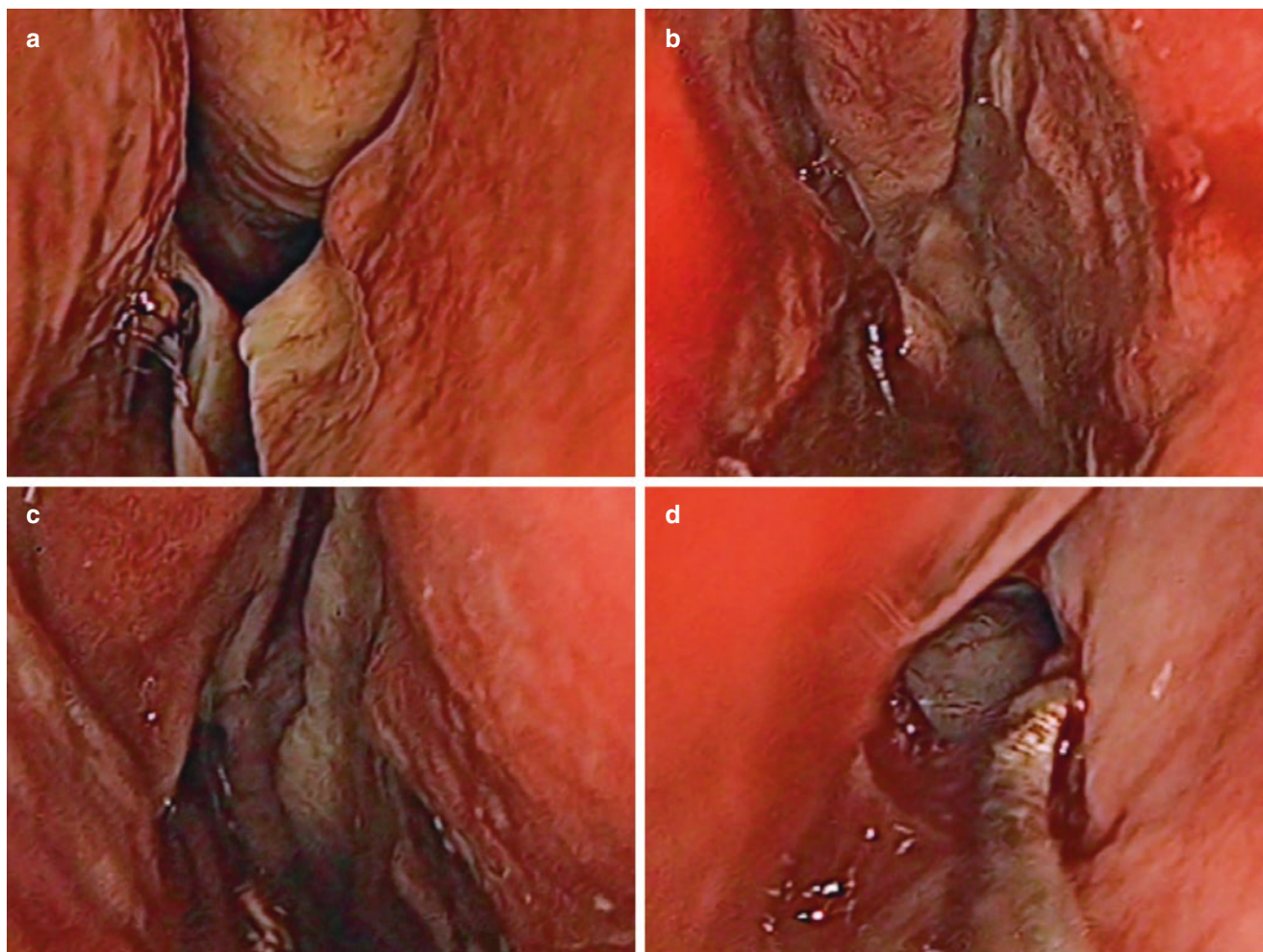
Fig. 7 (**a**, **b**) In the right nostril, the inferior and middle turbinates are displaced laterally to widen the surgical corridor. (**c**, **d**) Identification and initial opening of the ostium of the sphenoid sinus

the inferior third of the clivus superiorly and the C2 vertebral body inferiorly, and the lateral margin of the surgical exposure included the lateral masses of the C1 vertebra. Skeletonization of the anterior arch of C1 and the odontoid process was then carried out in a subperiosteal fashion. The lowest part of the clivus and the C1 anterior arch were then removed [17].

We checked the correct surgical position with the navigation system. A 3-mm coarse diamond burr was used to enter the anterior cortex of the odontoid process (extra-long high-speed microdrill; The Anspach Effort, Inc., Palm Beach Gardens, FL, USA). We proceeded with excision of pathological tissue between the odontoid process and the dura of the pontomedullary junction. An ultrasonic bone curette was then used to remove the tip of the odontoid process (Sonopet Omni ultrasonic surgical system; Stryker, Inc., Kalamazoo, MI, USA). Finally, the residual shell of the odontoid process could be removed by sectioning of the apical and alar ligaments, and separation of the process from adhesions to surrounding tissues [18].

Exposition of the dura anterior to the pontomedullary junction that was covered by inflammatory tissue. At the end of the procedure, image guidance was helpful for assessment of the effectiveness of the decompression. Furthermore, the integrity and the pulsatility of the dura were checked to rule out the risk of cerebrospinal fluid (CSF) leakage.

After the procedure, the inverted U-shaped mucosal naso-pharyngeal flap that had been harvested at the beginning of the procedure was retrieved to cover the surgical cavity and fixed with fibrin glue. A Foley catheter was used to hold it in place for 2 days to promote the healing process. Both nostrils were packed with nasal swabs.

Discussion

'Craniovertebral junction' is a collective term that refers to the occipital bone, atlas and axis with supporting ligaments and membranes that provide stability and mobility to this
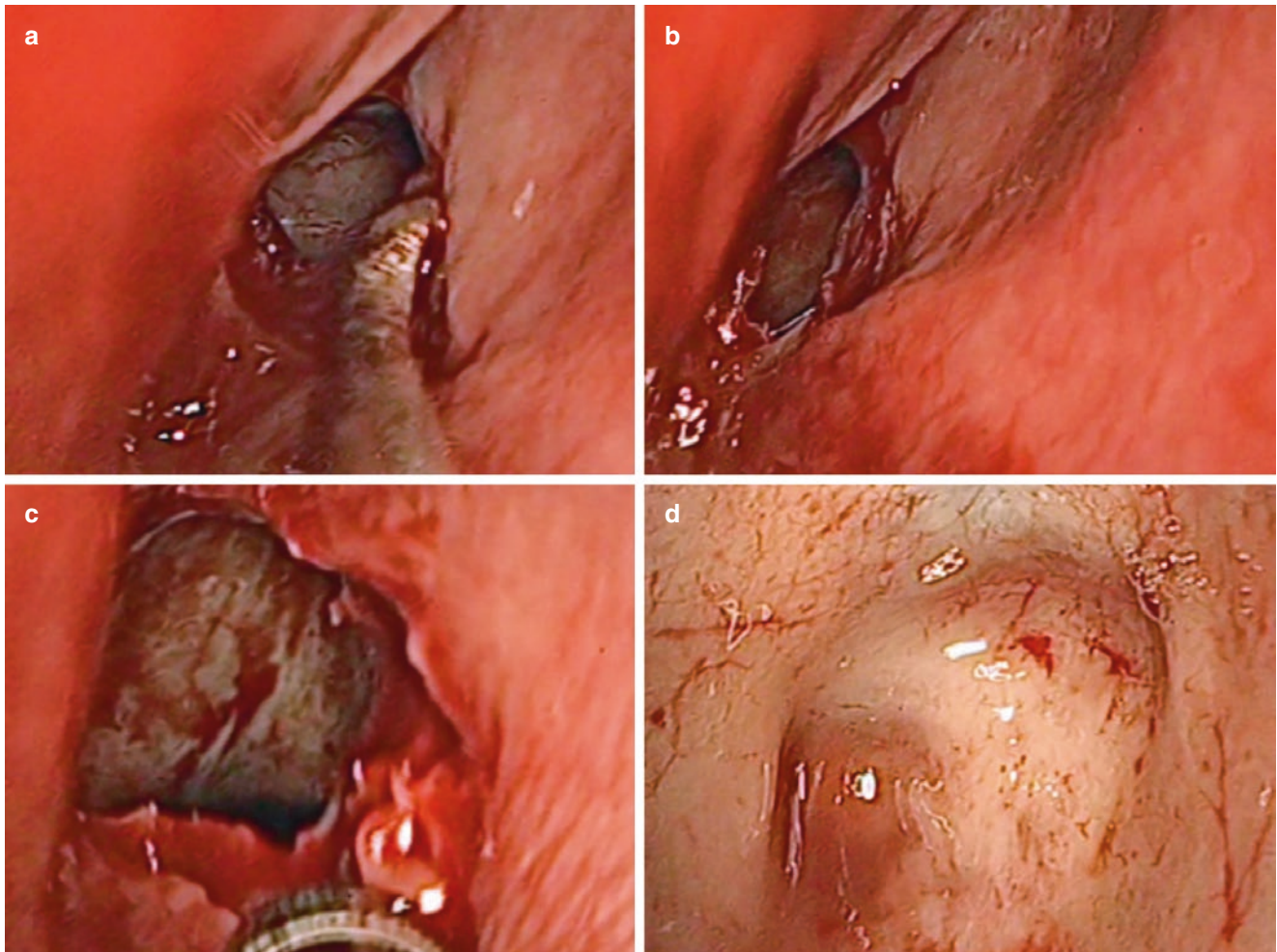
Fig. 8 (**a**, **b**) Opening of the ostium of the sphenoid sinus. (**c**, **d**) Identification of the sphenoid sinus and clivus

critical crossroads of the central nervous system at the brainstem transition to the spinal cord. Different surgical approaches have been described for exposing the CVJ, depending on the location of the pathology. If irreducible ventral compression of the brainstem occurs, an anterior route is the gold standard for obtaining straightforward access to the lesion without the need for neural tissue retraction [19]. The transoral, endonasal and transcervical approaches represent the three main options for performing odontoidectomy [4, 5, 8, 20]. The first approach to be reported was the transoral–transpharyngeal route to the ventral CVJ, described by Kanavel in 1917 [21]. Despite the wide surgical exposition (from the clivus to C2–C3) provided by this approach, it carries the risk of bacterial contamination, prolonged postoperative intubation, nasogastric tube feeding, tongue swelling and nasopharyngeal incompetence after transoral surgery [22]. The refinement of transsphenoidal endoscopic approaches to midline skull base lesions has led to the introduction of an endonasal route as a less invasive approach to the CVJ [23–25]. The extended endonasal approach exploits an anatomical corridor to the

odontoid process, involving only a small incision in the nasopharynx and sparing palate integrity, without exposure to saliva and oropharyngeal bacteria, and therefore with a theoretically lower infectious risk [24, 26]. The endoscopic approach can provide access to the entire skull base, extending from the anterior cranial fossa to the body of C2 on the midline. The lateral exposure is limited here by the Eustachian tube, medial pterygoid plates and paraclival internal carotid arteries (ICAs). The muscles of the ventral CVJ are thin and have an avascular plane on the midline that can be used to retract them laterally or remove them as a U-shaped flap for later reconstruction. The anterior tubercle of C1 is a useful midline landmark, which can be confirmed with image guidance. A cadaver study by Baird et al. [27], comparing the endonasal, transoral and transcervical endoscopic approaches, showed that the EEA offers a shorter distance to the surgical target. Moreover, with the endonasal approach, the trajectory is entirely top down; thus, it is favourable to achieve better control of the drill and advantageous for detaching the ligaments while performing clivus and odontoid resection [27]. In addition, the endoscope provides supe-
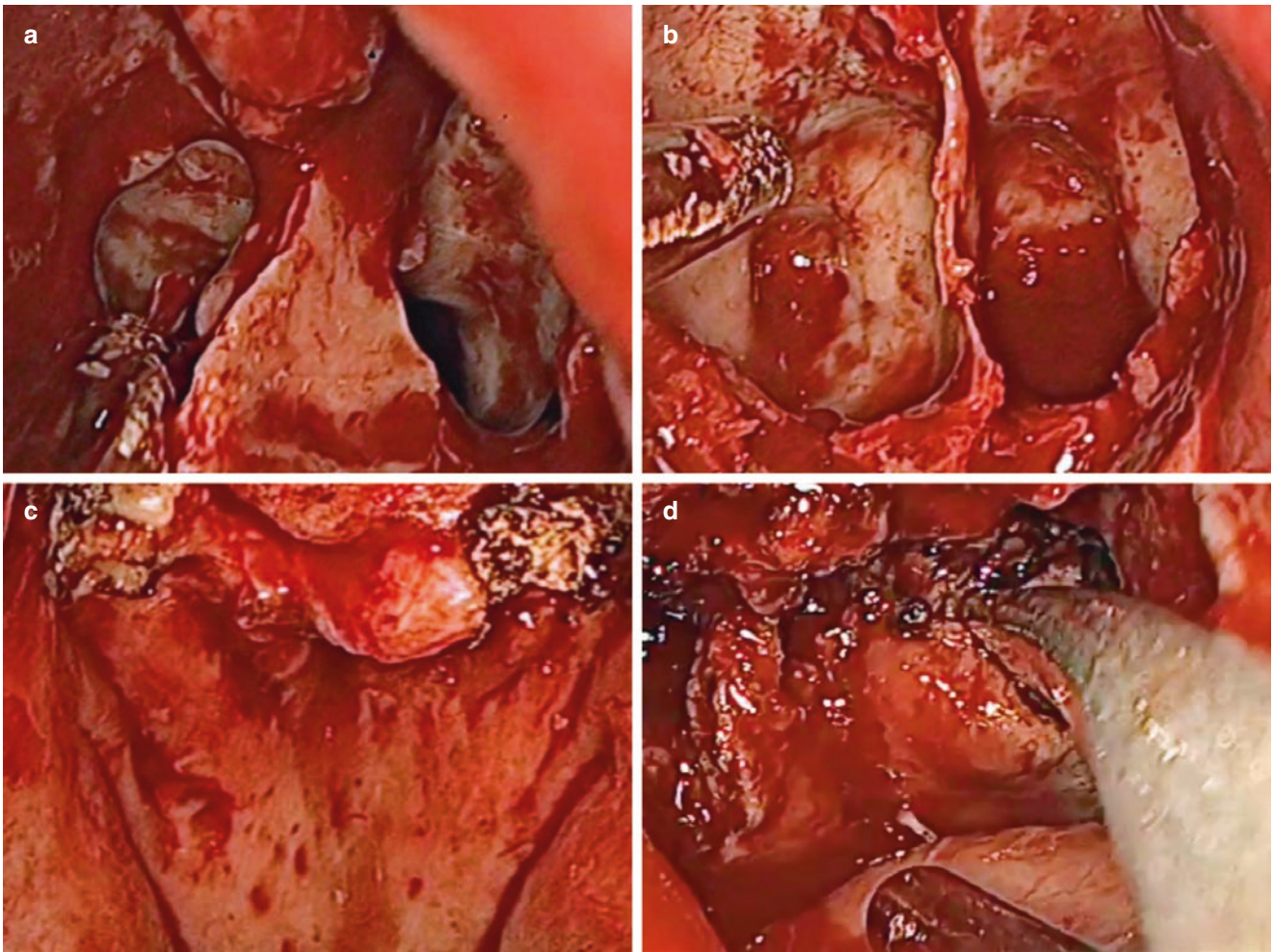
Fig. 9 (**a**) Rostrum of the sphenoid bone. (**b**) Clivus and paraclival carotid. (**c**, **d**) Inverted U-shaped flap of nasopharyngeal mucosa and muscular layers harvested with the laser

rior visualization and a larger optical field than the microscope does, which has turned out to be particularly advantageous in this deep surgical field. As highlighted by Ponce-Gómez et al. [3] in the odontoidectomy setting, the views differ between the endoscope and the microscope, and in such a narrow working area, movements are more fluent and faster with an endoscope. 3D endoscopes, which provide depth perception, may further improve the precision and safety of surgical manoeuvres [11, 15].

Maintenance of CVJ stability is another major issue to consider while performing surgical procedures at this level. Preservation of anterior C1 arch continuity by resection of only the odontoid process and pathological tissue—when feasible—reduces the risk of spinal biomechanical instability and the need for posterior fusion [9, 15]. One of the main criticisms of the EEA to the upper cervical spine is the limited exposure inferiorly. The K line, also known as the nasopalatine line (NPL), provides a window of caudal exposure inferior to the horizontal plane of the hard palate. As De Almeida et al. [26] demonstrated in their work describing extrapolation of the NPL to the vertebral column, the most inferior limit of dissection with endoscopic instruments is about 8.9 mm above the base of the C2 vertebral body. These findings suggest that while removal of the C2 body cannot be performed with the EEA, odontoidectomy usually is feasible with the EEA. It is currently thought that the surgical approach has to be tailored to the unique anatomical setting of each patient and the features of the lesion. On the basis of our own surgical experience, drilling of the inferior nasal spine, located between the soft and the hard palate, can be useful to widen the route of access to the CVJ, to gain more caudal access [16]. Further inferior dissection may require the use of angled instruments or a transoral approach [26]. Another drawback of the EEA may be the steep and long learning curve that this complex approach requires. Last—but not least—for a skull base neurosurgeon, being familiar with the EEA means not only being able to perform it but also being able to deal effectively with the complications that may derive from this approach.

A recent review by Shriver et al. [6] stated that postoperative CSF leakage rates are higher after the EEA than after the transoral approach. This systematic review, comparing complications associated with transoral and transnasal odontoidectomy, reported intraoperative CSF leakage rates of 0.3% and 30%, respectively, and postoperative CSF leakage rates of 0.8% and 5.2%, respectively. CSF leaks, if not properly treated, may lead to meningitis. Therefore, a skull base neurosurgeon dealing with the EEA should be prepared to deal with complex CSF leaks.

We performed the approach using a Visionsense III 3D endoscope. The relative importance of the 3D view depends on the relative increase in the depth of field it provides in comparison with a 2D endoscope. In 2012, Castelnuovo et al. [28] described one case of transnasal resection of an anterior skull base malignancy with a 3D endoscope. They reported that the surgeons were able to recognize and manage anatomical structures, and control bleeding easily, thanks to use of a bimanual technique and 3D visualization. Probably the most fascinating potential of 3D vision is the ability to control the anatomical structures that are present but not usually and easily visible. The addition of depth perception allows us to overcome the limitations of 2D, making the new 3D endoscopic system an ideal tool for a wide range of procedures. Finally, the accuracy of the visualization of the anatomical structures and their relationships makes the 3D endoscope a versatile tool, which entails a shorter learning curve than the traditional 2D endoscope [12].

Conclusion

The endoscopic endonasal route to the odontoid process has proven to be a feasible, safe and well-tolerated procedure. Anatomical study is mandatory for better understanding of the three-dimensional anatomy of the craniovertebral junction (CVJ) and relation of critical neurovascular structures to specific bony and muscular landmarks. Endoscopic relation of CVJ anatomy is difficult and complex, and cadaver studies help to ensure safety and control during surgical procedures. Anatomical knowledge and dissection in the cadaver laboratory will help future neurosurgeons to develop approaches, facilitate safe surgery and reduce the current limitations of the endoscopic endonasal approach to the CVJ: the caudal exposure limited by nasal and palatine bony and soft tissues. The advantages of the endoscopic endonasal approach are the location of the incision (in the nasopharynx rather than in the oropharynx) and the wider, closer and brighter view provided by the endoscope. High-definition three-dimensional endoscopes, lasers and ultrasound bony curettes have been shown to be useful tools for this approach.

References

1. Lopez AJ, Scheer JK, Leibl KE, Smith ZA, Dlouhy BJ, Dahdale NS. Anatomy and biomechanics of the craniovertebral junction. Neurosurg Focus. 2015;38:E2.
2. Menezes AH, Traynelis VC. Anatomy and biomechanics of normal craniovertebral junction (a) and biomechanics of stabilization (b). Childs Nerv Syst. 2008;24:1091–100.
3. Ponce-Gómez JA, Ortega-Porcayo LA, Soriano-Barón HE, Sotomayor-González A, Arriada-Mendicoa N, Gómez-Amador JL, Palma-Díaz M, Barges-Coll J. Evolution from microscopic transoral to endoscopic endonasal odontoidectomy. Neurosurg Focus. 2014;37(4):E15.
4. Dickman CA, Crawford NR, Brantley A, Sonntag V. Biomechanical effects of transoral odontoidectomy. Neurosurgery. 1995;36(6):1146–53.
5. Naderi S, Crawford NR, Melton MS, et al. Biomechanical analysis of cranial settling after transoral odontoidectomy. Neurosurg Focus. 1999;6:E7.
6. Shriver MF, Kshettry VR, Sindwani R, Woodard T, Benzel EC, Recino PF. Transoral and transnasal odontoidectomy complications: a systematic review and meta-analysis. Clin Neurol Neurosurg. 2016;148:121–9.
7. Nayak JV, Gardner PA, Vescan AD, Carrau RL, Kassam AB, Snyderman CH. Experience with the expanded endonasal approach for resection of the odontoid process in rheumatoid disease. Am J Rhinol. 2007;21:601–6.
8. Steinmetz MP, Mroz TE, Benzel EC. Craniovertebral junction: biomechanical considerations. Neurosurgery. 2010;66(3 Suppl):7–12.
9. A Gladi M, Iacoangeli M, Specchia N, Re M, Dobran M, Alvaro L, Moriconi E, Scerrati M. Endoscopic transnasal odontoid resection to decompress the bulbo-medullary junction: a reliable anterior minimally invasive technique without posterior fusion. Eur Spine J. 2012;21(Suppl 1):S55–60.
10. Magrini S, Pasquini E, Mazzatenta D, Frank G, et al. Endoscopic endonasal odontoidectomy in a patient affected by Down syndrome: technical case report. Neurosurgery. 2008;63:e373–4.
11. Altieri R, Tardivo V, Pacca P, Pennacchietti V, Penner F, Garbossa D, Ducati A, Garzaro M, Zenga F. 3D HD endoscopy in skull base surgery: from darkness to light. Surg Technol Int. 2016;29: 359–65.
12. Pennacchietti V, Garzaro M, Grottoli S, Pacca P, Garbossa D, Alessandro D, Zenga F. Three-dimensional endoscopic endonasal approach and outcomes in Sellar lesions: a single-center experience of 104 cases. World Neurosurg. 2016;89:121–5.
13. Cavallo LM, Cappabianca P, Messina A, Esposito F, Stella L, de Divitiis E, et al. The extended endoscopic endonasal approach to the clivus and cranio-vertebral junction: anatomical study. Childs Nerv Syst. 2007;23:665–71.
14. Cavallo LM, Messina A, Cappabianca P, Esposito F, de Divitiis E, Gardner P, Tschabitscher M. Endoscopic endonasal surgery of the midline skull base: anatomical study and clinical considerations. Neurosurg Focus. 2005;19:1–14.
15. Zenga F, Marengo N, Pacca P, Pecorari G, Ducati A. C1 anterior arch preservation in transnasal odontoidectomy using three-dimensional endoscope: a case report. Surg Neurol Int. 2015;6:192.

16. Zenga F, Pacca P, Tardivo V, Pennacchietti V, Garbossa D, Pecorari G, Ducati A. Endoscopic endonasal approach to the odontoid pathologies. World Neurosurg. 2016;89:394–403.
17. Agrawal A, Reyes PM. A novel technique of odontoidoplasty and C1 arch reconstruction: anatomical and biomechanical basis. Neurosurgery. 2011;68(1 Suppl Operative):103–13.
18. Zenga F, Villaret AB, Fontanella MM, Nicolai P. Endoscopic trans-nasal odontoidectomy using ultrasonic bone curette: technical case report. Neurol India. 2013;61:69–72.
19. Jhawar S, Nunez M, Pacca P, Voscoboinik DS, Truong H. Craniovertebral junction 360°: a combined microscopic and endoscopic anatomical study. J Craniovertebr Junction Spine. 2016;7(4):204.
20. Dasenbrock HH, Clarke MJ, Bydon A, Wolinsky J-P, et al. Endoscopic image-guided transcervical odontoidectomy: out-comes of 15 patients with basilar invagination. Neurosurgery. 2012;70:351–60.
21. Kanavel AB. Bullet located between the atlas and the base of the skull: technique of removal through the mouth. Surg Clin Chicago. 1917;1:361–6.
22. Crockard HA. Transoral surgery: some lessons learned. Br J Neurosurg. 1995;9:283–93.
23. Alfieri A, Jho HD, Tschabitscher M. Endoscopic endonasal approach to the ventral cranio-cervical junction: anatomical study. Acta Neurochir (Wien). 2002;144:219–35.
24. Kassam AB, Snyderman C, Gardner P, Carrau R, Spiro R. The expanded endonasal approach: a fully endoscopic transnasal approach and resection of the odontoid process: technical case report. Neurosurgery. 2005;57(Suppl 1):E213.
25. Messina A, Bruno MC, Coste A, Cavallo LM, de Divittis E, Cappabianca P, Tschabitscher M. Pure endoscopic endonasal odon-toidectomy: anatomical study. Neurosurg Rev. 2007;30(3):189–94.
26. De Almeida JR, Zanation AM, Snyderman CH, Carrau RL, Prevedello DM, Gardner PA, Kassam AB. Defining the nasopalatine line: the limit for endonasal surgery of the spine. Laryngoscope. 2009;119:239–44.
27. Baird CJ, Conway JE, Sciubba DM, Prevedello DM, Quiñones-Hinojosa A, Kassam AB. Radiographic and anatomic basis of endo-scopic anterior craniocervical decompression: a comparison of endonasal, transoral, and transcervical approaches. Neurosurgery. 2009;65(6 Suppl):158–64.
28. Castelnuovo P, Battaglia P, Bignami M, Dallan I. Endoscopic transnasal resection of anterior skull base malignancy with a novel 3D endoscope and neuronavigation. Acta Otorhinolaryngol Ital. 2012;32:189–91.